Elastically Deformable Models

Demetri Terzopoulos[†]
John Platt[‡]
Alan Barr[‡]
Kurt Fleischer[†]

[†]Schlumberger Palo Alto Research, 3340 Hillview Avenue, Palo Alto, CA 94304
[‡]California Institute of Technology, Pasadena, CA 91125

Abstract: The theory of elasticity describes deformable materials such as rubber, cloth, paper, and flexible metals. We employ elasticity theory to construct differential equations that model the behavior of non-rigid curves, surfaces, and solids as a function of time. Elastically deformable models are active: they respond in a natural way to applied forces, constraints, ambient media, and impenetrable obstacles. The models are fundamentally dynamic and realistic animation is created by numerically solving their underlying differential equations. Thus, the description of shape and the description of motion are unified.

Keywords: Modeling, Deformation, Elasticity, Dynamics, Animation, Simulation
CR categories: G.1.8—Partial Differential Equations; I.3.5—Computational Geometry and Object Modeling (Curve, Surface, Solid, and Object Representations); I.3.7—Three-Dimensional Graphics and Realism

1. Introduction

Methods to formulate and represent instantaneous shapes of objects are central to computer graphics modeling. These methods have been particularly successful for modeling rigid objects whose shapes do not change over time. This paper develops an approach to modeling which incorporates the physically-based dynamics of flexible materials into the purely geometric models which have been used traditionally. We propose models based on elasticity theory which conveniently represent the shape and motion of deformable materials, especially when these materials interact with other physically-based computer graphics objects.

1.1. Physical Models versus Kinematic Models

Most traditional methods for computer graphics modeling are kinematic; that is, the shapes are compositions of geometrically or algebraically defined primitives. Kinematic models are passive because they do not interact with each other or with external forces. The models are either stationary or are subjected to motion according to prescribed

trajectories. Expertise is required to create natural and pleasing dynamics with passive models.

As an alternative, we advocate the use of active models in computer graphics. Active models are based on principles of mathematical physics [5]. They react to applied forces (such as gravity), to constraints (such as linkages), to ambient media (such as viscous fluids), or to impenetrable obstacles (such as supporting surfaces) as one would expect real, physical objects to react.

This paper develops models of deformable curves, surfaces, and solids which are based on simplifications of elasticity theory. By simulating physical properties such as tension and rigidity, we can model static shapes exhibited by a wide range of deformable objects, including string, rubber, cloth, paper, and flexible metals. Furthermore, by including physical properties such as mass and damping, we can simulate the dynamics of these objects. The simulation involves numerically solving the partial differential equations that govern the evolving shape of the deformable object and its motion through space.

The dynamic behavior inherent to our deformable models significantly simplifies the animation of complex objects. Consider the graphical representation of a coiled telephone cord. The traditional approach has been to represent the instantaneous shape of the cord as a mesh assembly of bicubic spline patches or polygons. Making the cord move plausibly is a nontrivial task. In contrast, our deformable models can provide a physical representation of the cord which exhibits natural dynamics as it is subjected to external forces and constraints.

1.2. Outline

The remainder of the paper develops as follows: Section 2 discusses the connections of our work to other physical models in computer graphics. Section 3 gives differential equations of motion describing the dynamic behavior of deformable models under the influence of external forces. Section 4 contains an analysis of deformation and defines deformation energies for curve, surface, and solid models. Section 5 lists various external forces that can be applied to deformable models to produce animation. Section 6 describes our implementation of deformable models. Section 7 presents simulations illustrating the application of deformable models. Section 8 discusses our work in progress.

2. Related Graphics Models

Interestingly, the classical spline representations of shape have characterizations based in elasticity theory [7]. However, in adopting splines as a representation of curve and surface shape, the graphics literature has deemphasized the physical basis of splines. The cubic interpolating spline, for instance, is an abstraction of the shape exhibited by a thin elastic beam (the elastica used in boat construction) whose minimal bending energy configuration may be characterized by a fourth-order differential equation. The elasticity theory perspective leads to generalized spline representations of curves, surfaces, and solids. Our work in this paper can be viewed as an extension, including physically-based dynamics, of the mixed-order generalized splines employed in computer vision by Terzopoulos [24].

Special purpose physical models have begun to capture the attention of the computer graphics community. Fluid mechanics was used by Peachey [20] and Fournier and Reeves [11] to model water waves, as well as Kajiya and von Herzen [17] and Yaeger et al. [28] for cloud simulation. Also, the physics of imaging has been applied to rendering [16, 15]. Weil [26] used catenaries to approximate cloth, while Feynman [10] used a more sophisticated thin plate flexure model for the same purpose.

Terzopoulos [23] employed deformable models based on variational principles to reconstruct surfaces from scattered visual constraints. To create deformable models, Barr [3] subjected solid primitives to prescribed deformations using Jacobian matrices. Sederberg and Parry [21] imposed similar deformations to solids modeled as free-form surfaces. We extend these approaches by adding equations governing the evolution of deformations.

Our models are compatible with and complementary to the constraint-based modeling approach for rigid primitives proposed by Barzel and Barr [4], as well as with the dynamics-based approaches of Wilhelms and Barsky [27] and Armstrong and Green [1] to animating articulated rigid bodies. Finally, since computer vision is the inverse problem of computer graphics, the models presented in this paper are of value for reconstructing mathematical representations of non-rigid objects from their images [25].

3. Dynamics of Deformable Models

We begin the mathematical development by giving the equations of motion governing the dynamics of our deformable models under the influence of applied forces. The equations of motion are obtained from Newtonian mechanics and balance the externally applied forces with the forces due to the deformable model.

Let a be the intrinsic or material coordinates of a point in a body Ω. For a solid body, a has three components: $[a_1, a_2, a_3]$. Similarly, for a surface a = $[a_1, a_2]$, and a curve a = $[a_1]$. The Euclidean 3-space positions of points in the body are given by a time-varying vector valued function of the material coordinates $r(a, t)$ = $[r_1(a, t), r_2(a, t), r_3(a, t)]$. The body in its natural rest state (see Figure 1) is specified by $r^0(a) = [r_1^0(a), r_2^0(a), r_3^0(a)]$.
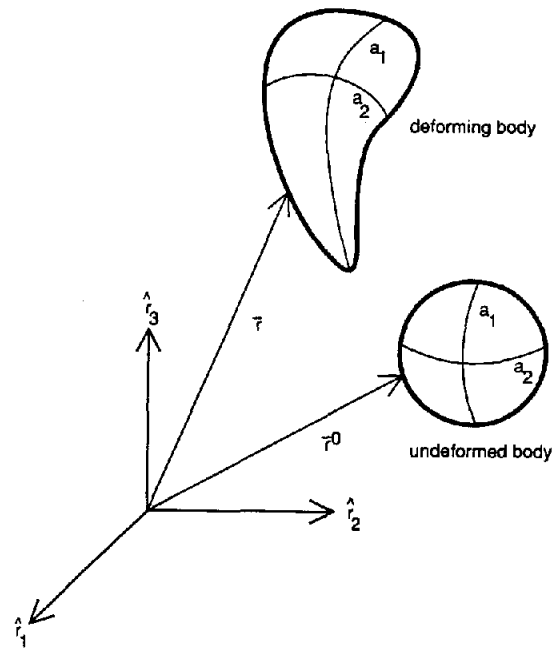

Figure 1. Coordinate systems.

The equations governing a deformable model's motion can be written in Lagrange's form [14] as follows:

$$\frac{\partial}{\partial t}\left(\mu \frac{\partial r}{\partial t}\right) + \gamma \frac{\partial r}{\partial t} + \frac{\delta \mathcal{E}(r)}{\delta r} = f(r, t), \qquad (1)$$

where $r(a, t)$ is the position of the particle a at time t, $\mu(a)$ is the mass density of the body at a, $\gamma(a)$ is the damping density, and $f(r, t)$ represents the net externally applied forces. $\mathcal{E}(r)$ is a *functional* which measures the net instantaneous potential energy of the elastic deformation of the body.

The external forces are balanced against the force terms on the left hand side of (1) due to the deformable model. The first term is the inertial force due to the model's distributed mass. The second term is the damping force due to dissipation. The third term is the elastic force due to the deformation of the model away from its natural shape.

The elastic force is conveniently expressed as $\delta \mathcal{E}(r)/\delta r$, a *variational derivative* of the potential energy of deformation $\mathcal{E}(r)$ (as approximated in equation 14). More information on variational derivatives can be found in textbooks on the calculus of variations [5, 13].

4. Energies of Deformation

This section develops potential energies of deformation $\mathcal{E}(r)$ associated with the elastically deformable models. These energies are employed to define the internal elastic forces of the models (see Section 6).

4.1. Analysis of Deformation

Elasticity theory involves the analysis of deformation [18, 12]. We will define measures of deformation using concepts from the differential geometry of curves, surfaces, and solids [8]. One requirement of our present approach is that the measures should be insensitive to rigid body motion since it imparts no deformation.

The shape of a body is determined by the Euclidean distances between nearby points. As the body deforms, these distances change. Let a and a + da be the material coordinates of two nearby points in the body. The distance between these points in the deformed body in Euclidean 3-space is given by

$$dl = \sum_{i,j} G_{ij} da_i da_j, \qquad (2)$$

where the symmetric matrix

$$G_{ij}(\mathbf{r}(a)) = \frac{\partial \mathbf{r}}{\partial a_i} \cdot \frac{\partial \mathbf{r}}{\partial a_j} \qquad (3)$$

is known as the metric tensor or first fundamental form [9] (the dot indicates the scalar product of two vectors).

Two 3-dimensional solids have the same shape (differ only by a rigid body motion) if their 3×3 metric tensors are identical functions of $a = [a_1, a_2, a_3]$. However, this no longer need be true when the body becomes infinitesimally thin in one or more of its dimensions.

Thus, the lengths between nearby points do not determine the shape of a surface, since curvature can be altered without affecting lengths. The fundamental theorem of surfaces [8] states that two surfaces have the same shape if their metric tensors G as well as their curvature tensors B are identical functions of $a = [a_1, a_2]$. The 2×2 matrices G and B are the first and second fundamental forms of the surface [9]. The components of the curvature tensor are

$$B_{ij}(\mathbf{r}(a)) = \mathbf{n} \cdot \frac{\partial^2 \mathbf{r}}{\partial a_i \partial a_j}, \qquad (4)$$

where $\mathbf{n} = [n_1, n_2, n_3]$ is the unit surface normal.

For the case of space curves, the metric and curvature tensors are scalars called the arc length $s(\mathbf{r}(a))$ and the curvature $\kappa(\mathbf{r}(a))$. Again, arc length and curvature do not entirely determine the shape of a space curve; the curve can twist. Thus, the fundamental theorem of curves [8] states that two curves have the same shape if their arc length, curvature, and torsion $\tau(\mathbf{r})$ are identical functions of $a = a$ [9].

4.2. Energies for Curves, Surfaces, and Solids

Using the above differential quantities, we now define potential energies of deformation for elastic curves, surfaces, and solids. These energies restore deformed bodies to their natural shapes, while being neutral with respect to rigid body motion (see Figure 2). Thus, the potential energy should be zero when the model is in its natural state, and the energy should grow larger as the model gets increasingly deformed away from its natural state.

natural shape

rigid body motion
zero energy

small deformation
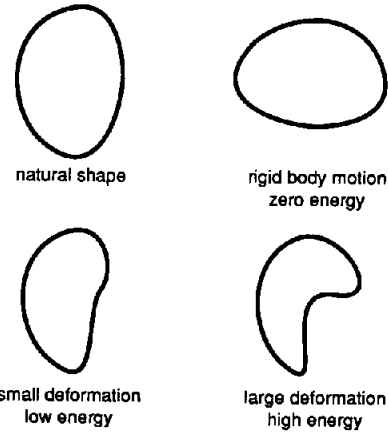low energy

large deformation
high energy

Figure 2. Energy of deformation.

A reasonable strain energy for elastic bodies is a norm of the difference between the fundamental forms of the deformed body and the fundamental forms of the natural, undeformed body. This norm measures the amount of deformation away from the natural state.

In the rest of the paper, the fundamental forms associated with the natural shapes of deformable bodies will be denoted by the superscript 0. For example,

$$G_{ij}^0 = \frac{\partial \mathbf{r}^0}{\partial a_i} \cdot \frac{\partial \mathbf{r}^0}{\partial a_j}. \qquad (5)$$

Thus, for a curve, we use the strain energy

$$\mathcal{E}(\mathbf{r}) = \int_\Omega \alpha(s - s^0)^2 + \beta(\kappa - \kappa^0)^2 + \gamma(\tau - \tau^0)^2 da \qquad (6)$$

where α, β, and γ are the amount of resistance of the curve to stretching, bending, and twisting, respectively. An analogous strain energy for a deformable surface in space is

$$\mathcal{E}(\mathbf{r}) = \int_\Omega \|G - G^0\|_\alpha^2 + \|B - B^0\|_\beta^2 \, da_1 da_2, \qquad (7)$$

where $\|\cdot\|_\alpha$ and $\|\cdot\|_\beta$ are weighted matrix norms. Similarly, a strain energy for a deformable solid is

$$\mathcal{E}(\mathbf{r}) = \int_\Omega \|G - G^0\|_\alpha^2 \, da_1 da_2 da_3. \qquad (8)$$

The deformation energies (6), (7), and (8) are zero for rigid motions, and they include the fewest partial derivatives necessary to restore the natural shapes of non-rigid curves, surfaces, and solids, respectively. However, higher-order derivatives can be included to further constrain the smoothness of the admissible deformations of these bodies [24].

5. Applied Forces

Applying external forces to elastic models yields realistic dynamics. This section lists representative examples

of external forces, including the effects of gravity, fluids, and collisions with impenetrable objects. The net external force $f(r, t)$ in (1) is the sum of the individual external forces. Various types of external forces, each a vector function of r, are presented below.

A gravitational force acting on the deformable body is given by

$$f_{gravity} = \mu(a)g, \qquad (9)$$

where $\mu(a)$ is the mass density and g is the gravitational field.

A force that connects a material point a_0 to a point in world coordinates $r_0 = [x_0, y_0, z_0]$ by an ideal Hookean spring is

$$f_{spring} = k(r_0 - r(a_0)), \qquad (10)$$

where k is the spring constant.

The force on the surface of a body due to a viscous fluid is

$$f_{viscous} = c(n \cdot v)n, \qquad (11)$$

where c is the strength of the fluid force, $n(a)$ is the unit normal on the surface, and

$$v(a, t) = u - \frac{\partial r(a, t)}{\partial t} \qquad (12)$$

is the velocity of the surface relative to some constant stream velocity u. The force is a flow field projected onto the normal of the surface, is linear in the velocity, and models a viscous medium [2].

We simulate collision dynamics between elastic models and immobile impenetrable objects by creating a potential energy $c \exp(-f(r)/\epsilon)$ around each object, where f is the object's inside/outside function. The constants c and ϵ determine the shape of the potential and are chosen such that the energy becomes prohibitive if the model attempts to penetrate the object. The resulting force of collision is

$$f_{collision} = - \left(\frac{\nabla f(r)}{\epsilon} \exp \left(-\frac{f(r)}{\epsilon} \right) \cdot n \right) n, \qquad (13)$$

where $n(a)$ is the unit normal vector of the deformable body's surface. This force ignores frictional effects at contact points, but it is a straightforward matter to define friction forces which impede sliding motions along the object's surface.

Elastic bodies should not self-intersect as they deform. Self-intersection can be avoided by surrounding the surface of the object with a self-repulsive collision force. The repulsive force requires an implicit description of the surface of the object, which is only available locally in our models. Thus, each object decomposes into many small patches and the repulsive force computation can become expensive. However, greater efficiency may be obtained by placing the patches into hierarchical bounding boxes.

6. Implementation of Deformable Models

To create animation with deformable models, the differential equations of motion are simulated numerically. We concentrate on the case of surfaces in order to illustrate the implementation of deformable models. Curves (solids)

represent a straightforward restriction (extension) of the discrete two-parameter equations developed in this section. Discrete equations of motion are sought that are tractable and stable. We first propose a simplification of the elastic forces $\delta \mathcal{E}(r)/\delta r$. The partial differential equation (1) is then discretized in space. Finally, the resulting system of coupled ordinary differential equations is integrated through time using standard techniques.

6.1. A Simplified Elastic Force

We will use a weighted matrix norm in (7) to obtain the following simplified deformation energy for a surface:

$$\mathcal{E}(r) = \int_\Omega \sum_{i,j=1}^2 \left(\eta_{ij} (G_{ij} - G_{ij}^0)^2 + \xi_{ij} (B_{ij} - B_{ij}^0)^2 \right) da_1 da_2, \qquad (14)$$

where $\eta_{ij}(a)$ and $\xi_{ij}(a)$ are weighting functions.

The first variational derivative $\delta \mathcal{E}(r)/\delta r$ of (14) can be approximated by the vector expression:

$$e(r) = \sum_{i,j=1}^2 -\frac{\partial}{\partial a_i} \left(\alpha_{ij} \frac{\partial r}{\partial a_j} \right) + \frac{\partial^2}{\partial a_i \partial a_j} \left(\beta_{ij} \frac{\partial^2 r}{\partial a_i \partial a_j} \right), \qquad (15)$$

where $\alpha_{ij}(a, r)$ and $\beta_{ij}(a, r)$ are constitutive functions describing the elastic properties of the material.

Now,

$$\alpha_{ij}(a, r) = \eta_{ij}(a) \left(G_{ij} - G_{ij}^0 \right). \qquad (16)$$

When α_{ij} is positive the surface wants to shrink in extent, and when α_{ij} is negative, it wants to grow. Thus, the α_{ij} are controlling surface tensions which minimize the deviation of the surface's actual metric from its natural metric G_{ij}^0. As $\eta_{ij}(a_0)$ is increased, the material's resistance to such deformation increases at material point a_0. η_{11} and η_{22} determine the resistance to length deformation along the coordinate directions, while $\eta_{12} = \eta_{21}$ determine the resistance to shear deformation.

Unfortunately, the calculus of variations applied to the second term in (14) yields unwieldy expressions. One alternative which follows by analogy to (16) is to use

$$\beta_{ij}(a, r) = \xi_{ij}(a) \left(B_{ij} - B_{ij}^0 \right). \qquad (17)$$

When β_{ij} is positive, the surface wants to be flatter, and when β_{ij} is negative, the surface wants to be more curved. Thus, β_{ij} are controlling surface rigidities which act to minimize the deviation of the surface's actual curvature from it's natural curvature B_{ij}^0. As $\xi_{ij}(a_0)$ is increased, the material becomes more resistant to such deformation at material point a_0. ξ_{11} and ξ_{22} determine the resistance to bending deformation along the coordinate directions, while $\xi_{12} = \xi_{21}$ determines the resistance to twist deformation.

To simulate a stretchy rubber sheet, for example, we make η_{ij} relatively small and set $\xi_{ij} = 0$. To simulate relatively stretch resistant cloth, we increase the value of η_{ij}. To simulate paper, we make η_{ij} relatively large and we introduce a modest value for ξ_{ij}. Springy metal is simulated by increasing the value of ξ_{ij}. The ability to set η and ξ independently at each material point a allows the intro-

duction of local singularities such as fractures and creases [24].

Note that for the special case where $\alpha_{12} = \alpha_{21} = 0$ and where α_{11}, α_{22}, and the β_{ij} are linearized so as to be independent of $\mathbf{r}$, we obtain the "thin plate surface under tension" [24]. The thin plate surface under tension further reduces to the traditional "spline under tension" in the case of curves.

6.2. Discretization

Expression (15) for the elastic force is continuous in the material coordinates of the deformable surface. For simulating the dynamics of the model, (15) can be discretized by applying finite element or finite difference approximation methods [19]. Discretization transforms the partial differential equation of motion (1) into a system of linked ordinary differential equations. We illustrate the discretization step using standard finite difference approximations.

The discrete representation of the unit square domain $0 \leq a_1, a_2 \leq 1$ on which the surface is defined is a regular $M \times N$ discrete mesh of nodes with horizontal and vertical inter-node spacings h_1 and h_2. The nodes are indexed by integers $[m,n]$ where $1 \leq m \leq M$ and $1 \leq n \leq N$. We approximate an arbitrary continuous vector function $\mathbf{u}(a_1, a_2)$ by the grid function $\mathbf{u}[m,n] = \mathbf{u}(mh_1, nh_2)$ of nodal variables.

The elastic force requires approximations to the first and second derivatives of the nodal variables. Given a grid function $\mathbf{u}[m,n]$, we first define the forward first difference operators

$$D_1^+(\mathbf{u})[m,n] = (\mathbf{u}[m+1,n] - \mathbf{u}[m,n])/h_1$$
$$D_2^+(\mathbf{u})[m,n] = (\mathbf{u}[m,n+1] - \mathbf{u}[m,n])/h_2 \qquad (18)$$

and the backward first difference operators

$$D_1^-(\mathbf{u})[m,n] = (\mathbf{u}[m,n] - \mathbf{u}[m-1,n])/h_1$$
$$D_2^-(\mathbf{u})[m,n] = (\mathbf{u}[m,n] - \mathbf{u}[m,n-1])/h_2. \qquad (19)$$

Using (18) and (19), we can define the forward and backward cross difference operators

$$D_{12}^+(\mathbf{u})[m,n] = D_{21}^+(\mathbf{u})[m,n] = D_1^+(D_2^+(\mathbf{u}))[m,n],$$
$$D_{12}^-(\mathbf{u})[m,n] = D_{21}^-(\mathbf{u})[m,n] = D_1^-(D_2^-(\mathbf{u}))[m,n], \qquad (20)$$

and the central second difference operators

$$D_{11}(\mathbf{u})[m,n] = D_1^-(D_1^+(\mathbf{u}))[m,n],$$
$$D_{22}(\mathbf{u})[m,n] = D_2^-(D_2^+(\mathbf{u}))[m,n]. \qquad (21)$$

Using the above difference operators, we can discretize the constitutive functions (16) and (17) as follows:

$$\alpha_{ij}[m,n] = \eta_{ij}[m,n](D_i^+(\mathbf{r})[m,n] \cdot D_j^+(\mathbf{r})[m,n] - G_{ij}^0[m,n]),$$

$$\beta_{ij}[m,n] = \xi_{ij}[m,n](\mathbf{n}[m,n] \cdot D_{ij}^{(+)}(\mathbf{r})[m,n] - B_{ij}^0[m,n]), \qquad (22)$$

where $\mathbf{n}[m,n]$ is the surface normal grid function and the $(+)$ superscript indicates that the forward cross difference operator is used when $i \neq j$.

The elastic force (15) can then be approximated by

$$\mathbf{e}[m,n] = \sum_{i,j=1}^{2} -D_i^-(\mathbf{p})[m,n] + D_{ij}^{(-)}(\mathbf{q})[m,n], \qquad (23)$$

where

$$\mathbf{p} = \alpha_{ij}[m,n]D_j^+(\mathbf{r})[m,n] \text{ and } \mathbf{q} = \beta_{ij}[m,n]D_{ij}^{(+)}(\mathbf{r})[m,n]. \qquad (24)$$

Jump discontinuities will generally occur in the surface: for example, at its external boundaries. However, a free (natural) boundary condition can be simulated by setting to zero the value of any difference operator D_i^+ or $D_{ij}^{(+)}$ in (24) involving $\mathbf{r}[m,n]$ on opposite sides of a boundary.

If the nodal variables comprising the grid functions $\mathbf{r}[m,n]$ and $\mathbf{e}[m,n]$ are collected into the MN dimensional vectors $\underline{\mathbf{r}}$ and $\underline{\mathbf{e}}$, (23) may be written in the vector form

$$\underline{\mathbf{e}} = \mathbf{K}(\underline{\mathbf{r}})\underline{\mathbf{r}} \qquad (25),$$

where $\mathbf{K}(\underline{\mathbf{r}})$ is an $MN \times MN$ matrix known as the *stiffness matrix*. Due to the local nature of the finite difference discretization, $\mathbf{K}$ has the desirable computational properties of sparseness and bandedness.

Consider, for simplicity, the case of time invariant mass density $\mu(\mathbf{a}, t) = \mu[a_1, a_2]$ and damping density $\gamma(\mathbf{a}, t) = \gamma[a_1, a_2]$ in (1). The resulting discrete densities are $\mu[m,n]$ and $\gamma[m,n]$. Let $\mathbf{M}$ be the *mass matrix*, a diagonal $MN \times MN$ matrix with the $\mu[m,n]$ variables as diagonal components, and let $\mathbf{C}$ be the *damping matrix* constructed similarly from $\gamma[m,n]$. The discrete form of the equations of motion (1) can be expressed in grid vector form using (25) by the following coupled system of second-order ordinary differential equations:

$$\mathbf{M}\frac{\partial^2 \underline{\mathbf{r}}}{\partial t^2} + \mathbf{C}\frac{\partial \underline{\mathbf{r}}}{\partial t} + \mathbf{K}(\underline{\mathbf{r}})\underline{\mathbf{r}} = \underline{\mathbf{f}}, \qquad (26)$$

where $\underline{\mathbf{f}}$ is the grid vector representing the discrete net external force.

6.3. Numerical Integration Through Time

To simulate the dynamics of an elastic model, the system of ordinary differential equations (26) is integrated through time. We integrate these equations using a numerical step-by-step procedure, which converts the system of nonlinear ordinary differential equations into a sequence of linear algebraic systems.

A time interval from $t = 0$ to $t = T$ is subdivided into equal time steps Δt, and the integration procedure computes a sequence of approximate solutions at times Δt, $2\Delta t, \ldots, t, t + \Delta t, \ldots, T$. Evaluating $\underline{\mathbf{e}}$ at $t + \Delta t$ and $\underline{\mathbf{f}}$ at t, and substituting the (second-order accurate) discrete time approximations

$$\frac{\partial^2 \underline{\mathbf{r}}}{\partial t^2} = (\underline{\mathbf{r}}_{t+\Delta t} - 2\underline{\mathbf{r}}_t + \underline{\mathbf{r}}_{t-\Delta t})/\Delta t^2$$
$$\frac{\partial \underline{\mathbf{r}}}{\partial t} = (\underline{\mathbf{r}}_{t+\Delta t} - \underline{\mathbf{r}}_{t-\Delta t})/2\Delta t \qquad (27)$$

into (26), we obtain the semi-implicit integration procedure

$$A_t \underline{r}_{t+\Delta t} = \underline{g}_t, \qquad (28)$$

where the matrix

$$A_t = K(\underline{r}_t) + \left(\frac{1}{\Delta t^2} M + \frac{1}{2\Delta t} C \right) \qquad (29)$$

and the effective force vector

$$\underline{g}_t = \underline{f}_t + \left(\frac{1}{\Delta t^2} M + \frac{1}{2\Delta t} C \right) \underline{r}_t + \left(\frac{1}{\Delta t} M - \frac{1}{2\Delta t} C \right) \underline{v}_t, \qquad (30)$$

with

$$\underline{v}_t = (\underline{r}_t - \underline{r}_{t-1})/\Delta t. \qquad (31)$$

This implicit procedure therefore evolves the dynamic solution from given initial conditions $\underline{r}_0$ and $\underline{v}_0$ by solving a time sequence of static equilibrium problems for the instantaneous configurations $\underline{r}_{t+\Delta t}$. Thus, the original nonlinear partial differential equation (1) has been reduced to a sequence of sparse linear algebraic systems (28), each of size proportional to MN, the number of nodes comprising the discrete deformable model.

We have used both direct methods, such as Choleski decomposition, and relaxation methods, such as the Gauss-Seidel method, to solve the sparse linear systems (28) (see [6]). Note that in the special case of linear elasticity, where α_{ij} and β_{ij} are constants independent of r, then $A_t = A$ is time-invariant, so a matrix decomposition solver need only perform a single initial decomposition of A, which significantly reduces the total amount of computation required. A detailed description of our linear equation solvers is beyond the scope of this paper.

7.   Simulation Examples

The following simulations have been selected to convey the broad scope of elastically deformable models.

Figure 3 shows two different static behaviors of an elastic surface. The surface is lifted by a spring attached to the rightmost corner and constrained at the remaining corners. Figure 3a simulates a thin plate, whose rest state is flat ($\eta_{ij} = 0$, $\beta_{ij} =$ positive constant). Figure 3b simulates a membrane resistant to stretch away from the prescribed metric G^0 (a prescribed-metric membrane) whose curvature is not regulated ($\eta_{ij} > 0$, $\xi_{ij} = 0$).

Figure 4 illustrates a ball resting on a supporting elastic solid. The solid has a prescribed metric tensor. The internal elastic force interacts with the collision force to deform the solid.

Figure 5 shows a shrink wrap effect. Figure 5a shows a model of a rigid jack. In Figure 5b, a spherical membrane is stretched to surround the jack. The membrane shrinks and the jack exerts an attractive force on the membrane until a balance is achieved with the collision force. The remaining figures are extracted from a motion sequence which simulates the shrinking membrane.

Figure 6 illustrates a simulation of a flag waving in the wind. The flag material is modeled as a fixed metric membrane. The wind is constant and its effect on the flag is modeled by the viscous force (11). The flag is fixed to
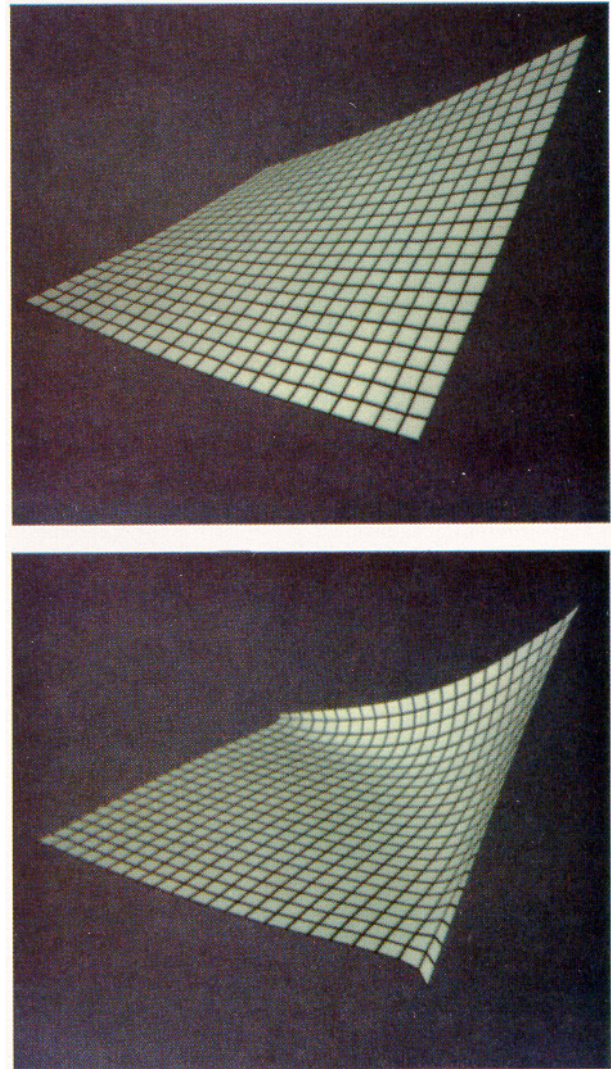

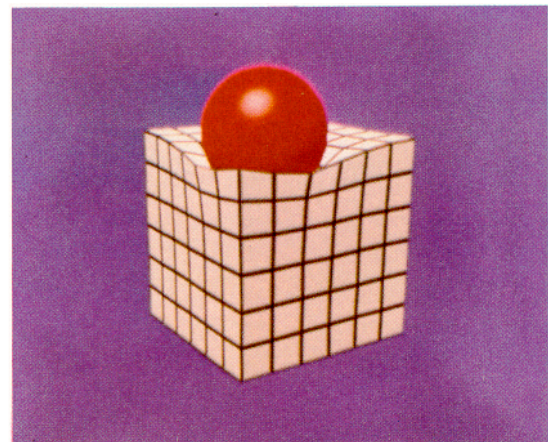**Figure 3.**   Lifting elastic surfaces.
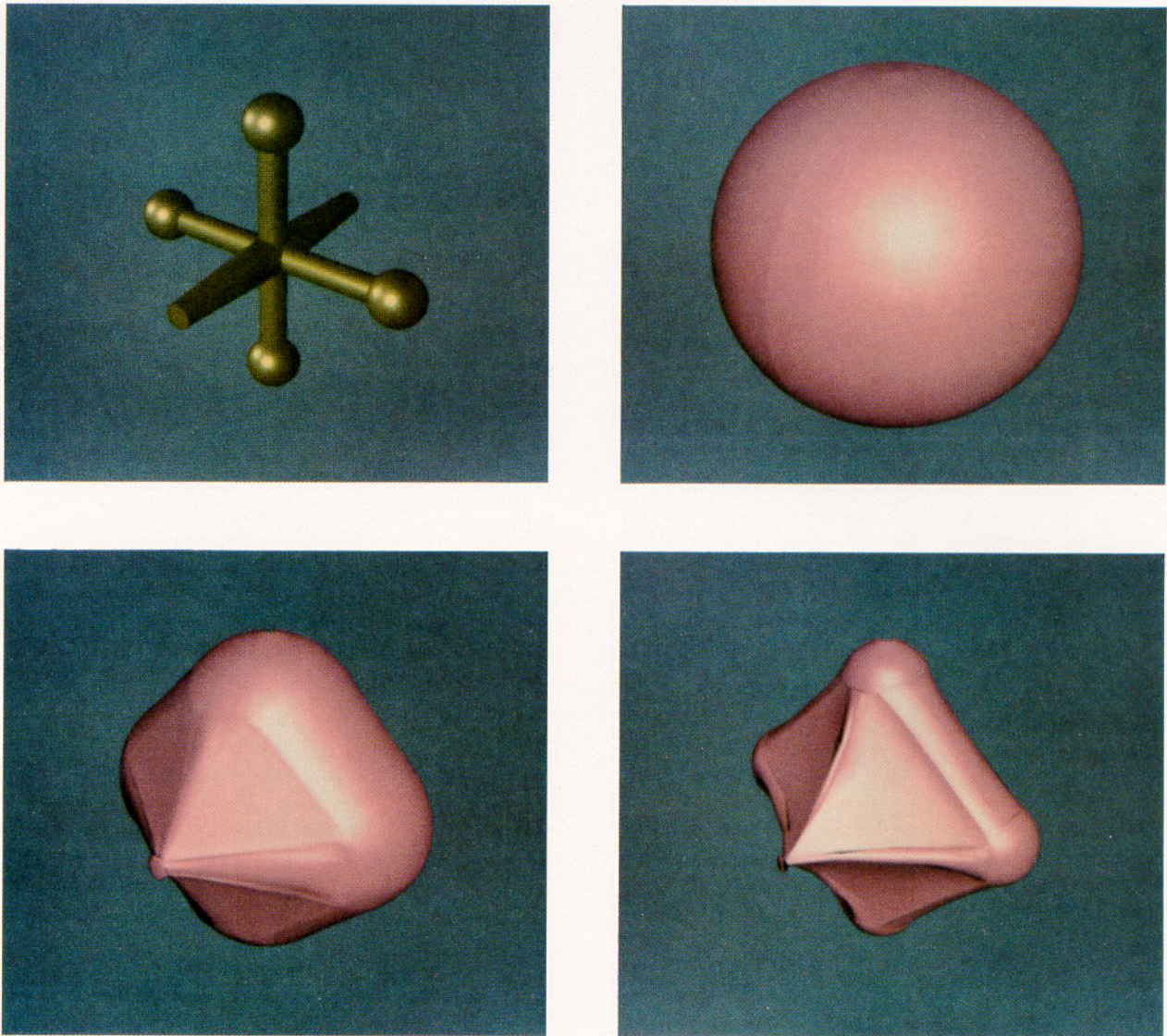

Figure 4.   Ball on a deformable solid.

Figure 5. Membrane shrinking around a jack.

a rigid flagpole along one of its edges by imposing a fixed-position (Dirichlet) boundary condition [19].

Figure 7 illustrates a simulation of a carpet falling onto two rigid bodies in a gravitational field. The carpet material is modeled as a prescribed-metric membrane with a small amount of plate rigidity ($\eta_{ij} > 0$, $\beta_{ij} > 0$). The carpet slides off the bodies due to the interaction between gravity and the repulsive collision force. The frictional component is due to the damping term in (1).

8. Work in Progress

We are currently experimenting with alternative formulations of deformable models. The elastic forces developed in this paper are nonlinear expressions involving 3-space position functions $\mathbf{r}$. In principle, we can use such expressions to simulate nonlinear elastic phenomena such as the

bending of shells [22]. Unfortunately, the discrete nonlinear approximations, especially the β_{ij} terms in (17), tend to be poorly conditioned numerically. One way to improve conditioning is to linearize the second term of (15) by making β_{ij} a function of $\mathbf{a}$, not of $\mathbf{r}$, resulting in the less general "thin plate" expression.

As an alternative, we have implemented linear elastic forces expressed in terms of the displacement $\mathbf{d} = \mathbf{r} - \mathbf{r}^0$ away from a reference 3-space configuration $\mathbf{r}^0$. The reference configuration $\mathbf{r}^0$ must, however, be allowed to undergo explicit rigid body motion, which amounts to solving the dynamical equations for rigid bodies [14]. The displacement formulation has allowed us to easily implement interesting visco-elasticity effects.

Another focus of our current work is on the topic of discretization and numerical solution of the deformable

Figure 6. Flag waving in a wind.

model equations. In the present paper we have employed finite difference discretization techniques. We are presently implementing more sophisticated discretizations using the finite element method [29]. We have also experimented with higher-order time integration procedures such as a fourth-order Runge-Kutta method [6]. Our results indicate that adaptive time-step control can be beneficial in increasing stability, especially during collisions with impenetrable objects. We are also developing a multigrid relaxation solver that promises to accelerate the solution of the very large discrete equations arising from detailed approximations [23].

9. Conclusion

This paper has proposed a class of elastically deformable models for use in computer graphics. Our goal has been to create models for non-rigid curves, surfaces, and solids that inherit the essential features of elastic materials, while still maintaining computational tractability. Because our models are physically-based, they are active: they respond to external forces and interact with other objects in a natural way. Our models yield realistic dynamics in addition to realistic statics; they unify the description of shape and motion. We therefore believe that physically-based modeling will prove to be an increasingly powerful technique for computer graphics animation.
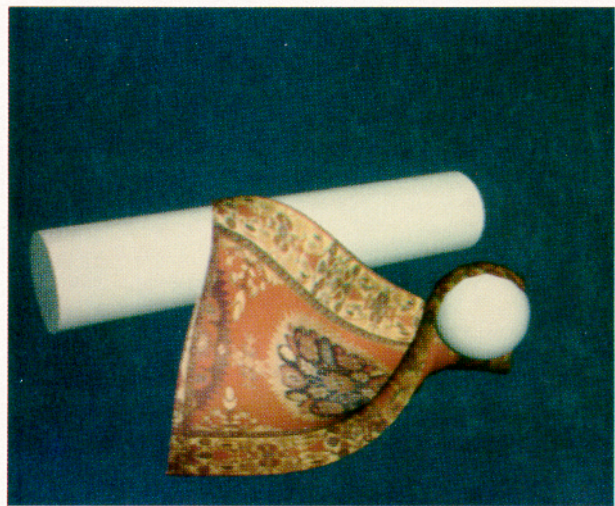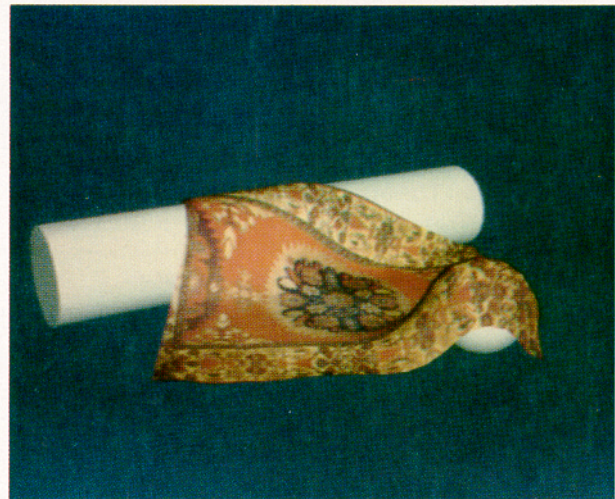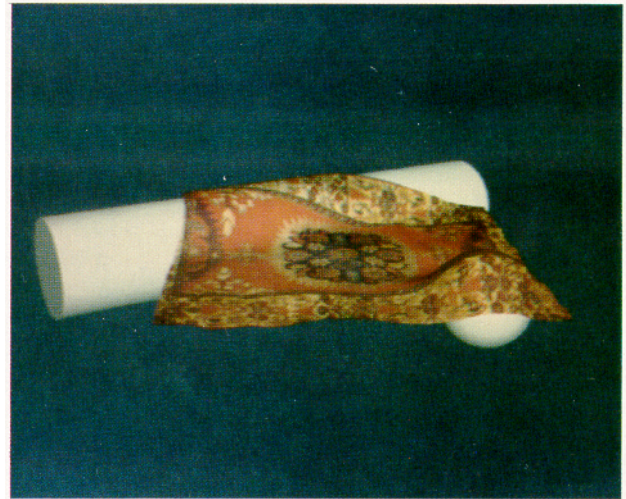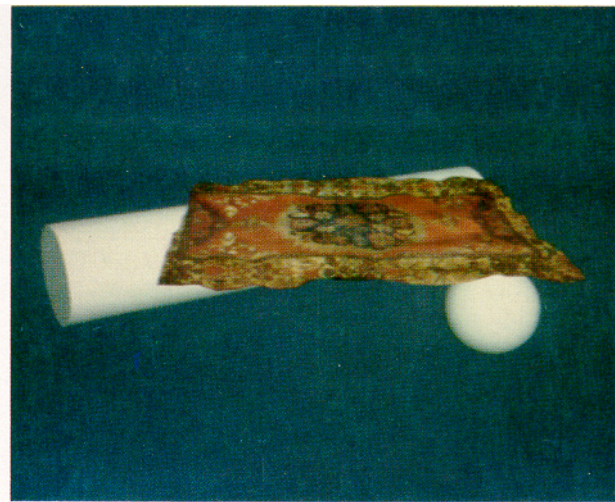
Figure 7. Persian carpet falling over immobile obstacles.

Acknowledgements

References

1. Armstrong, W.W., and Green, M., "The dynamics of articulated rigid bodies for purposes of animation," *Proc. Graphics Interface '85*, Montreal, Canada, 1985, 407–415.

2. Barr, A.H., Geometric Modeling and Fluid Dynamic Analysis of Swimming Spermatozoa, PhD thesis, Department of Mathematical Sciences, Rensselaer Polytechnic Institute, Troy, NY, 1983.

3. Barr, A.H., "Global and local deformations of solid primitives," *Computer Graphics*, 18, 3, 1984, (Proc. SIGGRAPH) 21-29.

4. Barzel, R., Dynamic Constraints, MSc thesis, Department of Computer Science, California Institute of Technology, Pasadena, CA, 1987.

5. Courant, R., and Hilbert, D., *Methods of Mathematical Physics*, Vol. I, Interscience, London, 1953.

6. Dahlquist, G., and Bjorck, A., *Numerical Methods*, Prentice–Hall, Englewood Cliffs, NJ, 1974.

7. de Boor, C., *A Practical Guide to Splines*, Springer–Verlag, New York, NY, 1978.

8. do Carmo, M.P., *Differential Geometry of Curves and Surfaces*, Prentice–Hall, Englewood Cliffs, NJ, 1974.

9. Faux, J.D., and Pratt, M.J., *Computational Geometry for Design and Manufacture*, Halstead Press, Horwood, NY, 1981.

10. Feynman, C.R., Modeling the Appearance of Cloth, MSc thesis, Department of Electrical Engineering and Computer Science, MIT, Cambridge, MA, 1986.

11. Fournier, A., and Reeves, W.T., "A simple model for ocean waves," *Computer Graphics*, 20, 4, 1986, (Proc. SIGGRAPH), 75–84.

12. Fung, Y.C., *Foundations of Solid Mechanics*, Prentice–Hall, Englewood Cliffs, NJ, 1965.

13. Gelfand, I.M., and Fomin, S.V., *Calculus of Variations*, Prentice–Hall, Englewood Cliffs, NJ, 1963.

14. Goldstein, H., *Classical Mechanics*, Addison-Wesley, Reading, MA, 1950.

15. Immel, D.S., Cohen, M.F., and Greenberg, D.P., "A radiosity method for non-diffuse environments," *Computer Graphics*, 20, 4, 1986, (Proc. SIGGRAPH), 133–142.

16. Kajiya, J.T., "The rendering equation," *Computer Graphics*, 20, 4, 1986, (Proc. SIGGRAPH), 143–150.

17. Kajiya, J.T., and von Herzen, B., "Ray tracing volume densities," *Computer Graphics*, 18, 3, 1984, (Proc. SIGGRAPH), 165–174.

18. Landau, L.D., and Lifshitz, E.M., *Theory of Elasticity*, Pergamon Press, London, UK, 1959.

19. Lapidus, L., and Pinder, G.F., *Numerical Solution of Partial Differential Equations in Science and Engineering*, Wiley, New York, NY, 1982.

20. Peachey, D.R., "Modeling waves and surf," *Computer Graphics*, 20, 4, 1986, (Proc. SIGGRAPH), 65–74.

21. Sederberg, T.W., and Parry, S.R., "Free-form deformation of solid geometric models," *Computer Graphics*, 20, 4, 1986, (Proc. SIGGRAPH), 151–160.

22. Stoker, J.J., *Nonlinear Elasticity*, New York, NY, 1968.

23. Terzopoulos, D., "Multilevel computational processes for visual surface reconstruction," *Computer Vision, Graphics, and Image Processing*, 24, 1983, 52–96.

24. Terzopoulos, D., "Regularization of inverse visual problems involving discontinuities," *IEEE Trans. Pattern Analysis and Machine Intelligence*, PAMI-8, 1986, 413–424.

25. Terzopoulos, D., "On matching deformable models to images: Direct and iterative solutions," *Topical Meeting on Machine Vision, Technical Digest Series, Vol. 12., Optical Society of America*, Washington, DC, 1987, 160–167.

26. Weil, J., "The synthesis of cloth objects," *Computer Graphics*, 20, 4, 1986, (Proc. SIGGRAPH), 49–54.

27. Wilhelms, J., and Barsky, B.A., "Using dynamic analysis to animate articulated bodies such as humans and robots," *Proc. Graphics Interface '85*, Montreal, Canada, 1985, 97–104.

28. Yaeger, L., Upson, C., and Myers, R., "Combining physical and visual simulation — creation of the planet Jupiter for the film "2010"," *Computer Graphics*, 20, 4, 1986, (Proc. SIGGRAPH), 85-94.

29. Zienkiewicz, O.C., *The Finite Element Method; Third edition*, McGraw–Hill, London, 1977.